Journal of Power Sources 196 (2011) 5494–5498

Contents lists available at ScienceDirect

Journal of Power Sources

journal homepage: www.elsevier.com/locate/jpowsour

Short communication

Alkaline anion-exchange polymer membrane with grid–plug microstructure for hydrogen fuel cell application

Xinhui Zhang[a], Siok Wei Tay[a], Zhaolin Liu[a], Liang Hong[a,b,*]

[a] Institute of Materials Research & Engineering, A*STAR (Agency for Science, Technology and Research), 3 Research Link, Singapore 117602, Singapore
[b] Department of Chemical & Biomolecular Molecular Engineering, National University of Singapore, 4 Engineering Drive 4, Singapore 117576, Singapore

ARTICLE INFO

Article history:
Received 22 September 2010
Received in revised form 2 December 2010
Accepted 11 December 2010
Available online 18 January 2011

Keywords:
Fuel cell
Anion-exchange membrane
Pore-filling
Ion-conducting phase

ABSTRACT

Porous polysulfone membrane, prepared by a phase-inversion technique, is filled with (3-acrylamidopropyl)trimethylammonium chloride and N,N′-methylenebisacrylamide via interfacial diffusion. The impregnated membrane is then subjected to UV-irradiation for polymerizing monomers that are entrapped in pore channels of the membrane. This in-situ polymerization engenders a grid–plug microstructure, where the grid is polysulfone and the plugs are an ion (OH^-) conducting phase. As the plugs are extensively interconnected and non-tortuous throughout the membrane matrix, the ion-conducting phase sustains a power density as high as 55 mW cm^{-2} at 60 °C. Thermal analysis indicates that the pore-filling condition affects the packing density of the plugs that in turn, impacts on ion transport flux.

1. Introduction

Fuel cell technology is set to play an important role in the 21st century given the prospects of contributing to clean and reliable power to meet the world's ever-growing demand for energy [1]. Among the different types of fuel cell systems, the proton exchange membrane fuel cell (PEMFC) is the most developed [2,3]. Despite having excellent performance stability, PEMFC still has several significant limitations that hinder its broad commercial application. The primary drawback lies in the inevitable use of expensive platinum and platinum-based electrodes [4,5]. The costly fluorinated PEM is another issue. In light of these shortcomings, the alkaline fuel cell (AFC) system offers a better solution, for instance it can employ cheaper non-noble metals, e.g., nickel, for the cathode [6]. In addition, the AFC possesses a more appropriate water management system [7] and good anodic kinetics [8,9]. These traits encourage attempts to develop anion-exchange membranes (AEM) with high OH^- ion-conductivity and strong mechanical properties [10,11]. Meanwhile, it also should be noted that the AFC has a smaller power density than a PEMFC because the OH^- ion, compared with the H^+ ion, presents a slower migration rate.

Most of AEMs fabricated to date are composed of a chain structure that consists of a hydrophobic backbone and randomly pendant quaternary ammonium groups [12–24]. Such chain structure, unless it has a hydrophobic and hydrophilic di-block pattern, often results in a membrane having inadequate mechanical strength and ionic conductivity. In this study, a special type of AEM matrix comprising a continuous grid and numerous plugs of an ion-conducting phase is developed. This matrix can successfully avoid the problem caused by random entanglement of the hydrophobic moiety and the ion-conducting phase. The ion-conducting phase, which is intimately plugged in a porous polysulfone (PSU) grid, is formed on polymerizing monomers in the pore channels. A large extent of interconnected OH^- transport branches is therefore laid out and provides the membrane with very high ion conductivity (10^{-1} S cm^{-1}). On the other hand, the strong PSU grid guarantees negligible dimensional expansion and prevents outflow of the anion-conducting phase upon impregnation of the membrane in aqueous solution.

2. Experimental

2.1. Chemicals

The following chemicals were used: polysulfone resins, PSU (P-3500, Udel®, Solvay Advanced Polymers); (3-acrylamidopropyl)-trimethylammonium chloride, ATC (Sigma–Aldrich, 75 wt.% water solution); N-methyl-2-pyrrolidone, NMP (Lab-Scan, 99.5%); ethanol (Merck, 99.9%); ammonium peroxodisulfate, $(NH_4)_2S_2O_8$ (Merck, ≥98%); and N,N′-methylenebisacrylamide (Sigma–Aldrich, 99%).

* Corresponding author at: Department of Chemical & Biomolecular Molecular Engineering, National University of Singapore, 4 Engineering Drive 4, Singapore 117576, Singapore. Tel.: +65 6516 5029; fax: +65 6779 1936.
E-mail address: chehongl@nus.edu.sg (L. Hong).

0378-7753/$ – see front matter © 2011 Elsevier B.V. All rights reserved.
doi:10.1016/j.jpowsour.2010.12.110

Table 1
Different compositions of monomer formula in the mixed solvent of NMP and H_2O used to fill PSU porous membrane.

Specimens	H_2O:NMP (v/v)	ATC:H_2O (w/w)
PSU-PATC(0.75)	4:1	0.75:1
PSU-PATC(1.0)	4:1	1.0:1
PSU-PATC(1.2)	4:1	1.2:1
PSU-PATC(1.5)	4:1	1.5:1

2.2. Synthesis of alkaline anion-exchange membranes

The polysulfone resins (3.2 g) were dispersed in 13.2 ml of NMP and ethanol (10/3.2, v/v) to form a homogenous viscous solution. The solution was then cast on a glass panel using a film applicator with a gate thickness of 120 μm. The glass panel was swiftly immersed in the coagulation bath ($V_{NMP} : V_{H_2O} = 1 : 1$) for 24 h. A white pre-membrane with a porous matrix was left behind on the panel after this inverse solvent extraction. It was then transferred into a specially formulated feed solution containing the ATC monomer, 1 wt.% of crosslinker MBA, and 5 wt.% of the UV initiator ammonium persulfate in a binary solution of NMP and H_2O. The composition of the feed solution is shown in Table 1. Subsequent soaking allows the monomers to diffuse into the pores. Next, the monomer-impregnated membrane was sandwiched between two glass plates, and the assembly was placed in a UV reactor (Hg lamps, 8×8 W) for 1 h to polymerize the entrapped monomers. The resulting membranes were then soaked in double distilled water at room temperature for 24 h to remove any unbound water-soluble species. The resulting membranes were soaked in dilute KOH solution for 24 h to convert the poly[(3-acrylamidopropyl)trimethylammonium chloride)], PATC, to the OH^- form, and finally washed thoroughly with water to remove any residual KOH.

The cryogenic ruptured surface of the membranes was examined by field emission scanning electron microscopy (JEOL JSM-6700F) operated at 5 kV. The relative amounts of nitrogen and sulfur present in PSU-PATC membranes (measured by using a Flash EA-112 elemental analyzer) is a useful indicator of the electrolyte loading, which is found to affect the ionic conductivity of the membranes. The water uptake of a membrane was determined as follows. A rectangular piece of membrane in the OH^- form was immersed in deionized water at room temperature for 24 h. The surface water was removed by pressing it between tissue paper and the weight was obtained immediately using an electronic balance to determine the wet weight, W_{wet}. The wet membrane was then dried in an oven at 100 °C for 24 h and weighed to determine the dry weight, W_{dry}. The water uptake was then calculated and the results are summarized in Table 2.

2.3. Thermal analysis of membranes

The thermal degradation profiles of the ion-conducting phase (PATC) and the grid (PSU) of the resulting membranes were recorded using a high resolution thermogravimetric analyzer (TA Instruments Q500). The samples were heated under a nitrogen purge (100 ml min^{-1}) to 800 °C at a heating rate of 10 °C min^{-1}. The glass transition behaviour of the composite membranes were measured with a differential scanning calorimeter (DSC 2920, TA Instrument). The samples (5–10 mg) were loaded individually in a pressure DSC cell and each test was conducted via a two-scan mode: in the first scan, the sample was heated from room temperature to 200 °C at a rate of 10 °C min^{-1} and cooled down to −20 °C using the same rate, then the same heating rate was applied to conduct the second scan (−10 to 250 °C). The energy–temperature profile produced by the second scan was recorded. The mechanical properties of membrane were tested with a mechanical analyzer (Instron 5569) using a 100 N load cell. Dumbbell-shaped specimens were cut following the standard ISO 527. The tensile properties of all film samples were measured in an air atmosphere at room temperature with a cross-head speed of 1 mm per min.

2.4. Assessment of membrane conductivity

The four-probe measurement method was used to measure the conductivity of the prepared membranes. The measurement kit consisted of two rectangular Teflon plates. On one plate, two parallel stainless strips, 2 cm apart, are entrenched as the outer current-carrying electrodes, and on the other plate two gold wires were fixed 1 cm apart as the inner potential-sensing electrodes. A measurement sample, 1 cm wide and 4 cm long, was sandwiched between the two plates. The impedance values were recorded using an Autolab instrument at galvanostatic mode with an a.c. current amplitude of 0.1 mA over a frequency range from 50 Hz to 1 MHz. As a result, a spectrum of frequency-dependent impedance, i.e., the Nyquist plot, was obtained and the resistance (R) due to OH^- ion transfer in the membrane could be read from the real part of the spectrum. The conductivity (C) was calculated using the formula $C = L/RWd$, where L is the distance between the two potential-sensing electrodes, and W and d the width and thickness of the membrane, respectively. The conductivity of the membranes was evaluated at temperatures up to 75 °C at 100% relative humidity. For each set temperature, a 30 min span was set to allow the measurement set-up to achieve steady-state before the impedance spectrum was recorded.

2.5. Fuel cell test

For hydrogen fuel cell tests, the membrane electrode assembly (MEA) was made by sandwiching the membrane between an anode sheet and a cathode sheet. Both electrode sheets were made from carbon paper (SGL, Germany) that was coated with a layer of platinum (20 wt.%) on carbon black (Alfa Aesar). The catalyst slurries were prepared by mixing ethanol, 5 wt.% polytetrafluoroethylene (PTFE) (Aldrich, 60 wt.% dispersion in water), and 95 wt.% Pt/C for the cathode ink or 95 wt.% Pt–Ru/C for anode ink. The average platinum loadings at the anode and cathode were 2 mg cm^{-2} and the effective area was 2 cm^2. Both H_2 and O_2 streams were applied at 1 bar pressure. The cathode was humidified by bubbling oxygen gas through a column of water immersed in a boiling water bath that aids the vaporizing process. Hydrogen was fed at a rate of 800 cm^3 min^{-1} and oxygen was delivered at a rate of 600 cm^3 min^{-1}.

3. Results and discussion

3.1. Solvent and interfacial diffusion

The porous pre-membrane PSU is fabricated by means of the phase-inversion technique [25,26]. The resultant liquid-borne PSU

Table 2
Specific heat of ionic glass transition of composite membranes[a].

Membranes	PSU-PATC(0.75)	PSU-PATC(1.0)	PSU-PATC(1.2)	PSU-PATC(1.5)
$\Delta H_{T_g}/\Delta H_{T_g}{}'$ [b]	1.0	2.4	2.5	1.2

[a] Determined by area of glass transition step in each T_g curve of Fig. 5. Samples for this measurement controlled to have the same mass.
[b] Relative specific heat value of composite membranes. ΔH_{T_g} is specific heat value of PSU-PATC(0.75).

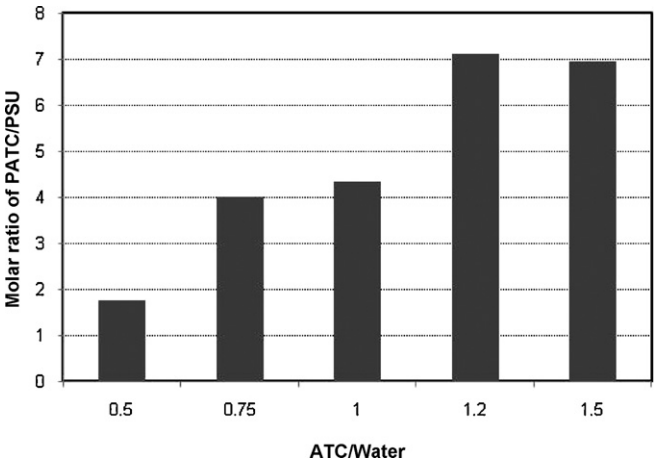

Fig. 1. Variation of ion-conducting phase (PATC) loading with use of different weight ratios of ATC to H_2O to prepare monomer formulae.

membrane must be used forthwith without evaporation of the solvent. When it was immersed in a solution of the monomer formula in NMP–H_2O, the monomers were driven by a concentration gradient and diffused into the interconnecting pore channels of the membrane. It is found that the volume ratio of NMP to H_2O used in the preparation of the monomer solution is crucial to the filling effect. A very low extent of polymerization of the monomer formula is found in the presence of a low content of NMP in the solution. An increase in the content of NMP in the feed leads to a large extent of gelation and hence diffusion into pore channels is impeded. Alternatively, when pure water is used, a lower filling effect is observed because water, being a non-solvent of PSU, causes the entries of pore channels to shrink. By comparing different filling extents, the solvent, $V_{NMP} : V_{H_2O} = 1 : 4$, is found to give the maximum filling degree. It is also noteworthy that the monomers that enter in the pore channels undergo gelation more rapidly since the liquid medium inside the pore-tubes and in PSU matrix has a far higher NMP content than that in the monomer solution.

In addition, the concentration of the monomers in the feed was increased to determine the highest possible level of loading (Table 1). The end point of soaking the PSU membrane in the feed is controlled by the emerging of a heavy extent of gelation. The monomer-loaded membranes are then subjected to UV-irradiation to enhance polymerization of the monomers entrapped in the pore channels. Based on the elemental analysis of purified composite membranes, the filling extent of the ion-conducting PATC phase can be obtained and is shown in Fig. 1. With increase in monomer concentration, the resulting membranes indeed show an increase in filling extent. An optimum concentration of monomer formula in the feed is obtained and is marked by ATC/H_2O = 1.2 (Table 1). In short, both the NMP content in the monomer solution and the concentration of ATC are crucial in the pore-filling result.

3.2. Characterization of the embedded ion-conducting phase

Thermogravimetric analysis (TGA) also verifies the presence of PATC (Fig. 2a) because PSU is thermally much more stable than PATC. The embedded PATC phase decomposes in two temperature ranges, namely, of 280–335 °C and 335–435 °C. By contrast, PSU remains stable up to 460 °C. As shown in Fig. 2b, the first structural degradation slope of the pure PATC starts at about 280 °C while that embedded in a PSU matrix takes place 40 °C earlier. This is considered to originate from the branched chains between crosslinked points. The branched chain structures are in general weaker than the linear chain structure because it contains a larger average chain–chain distance and many tertiary or quaternary carbon atoms [27].

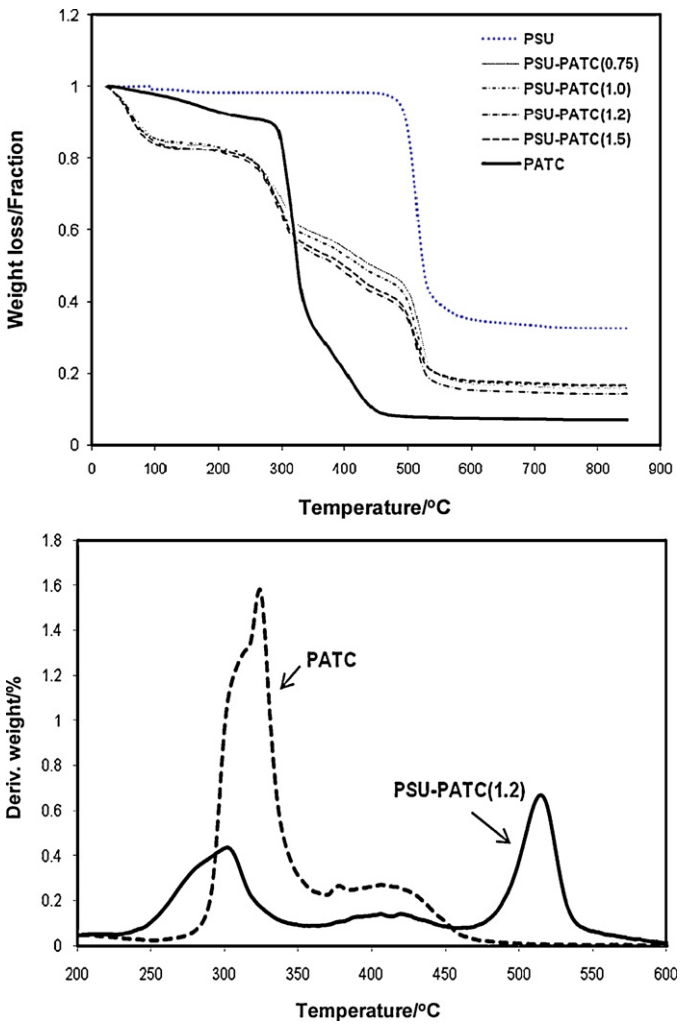

Fig. 2. (a) TGA thermographs of PSU porous substrate, PATC and PSU-PATC composite polymer membranes; (b) derivative profiles of PATC and PSU-PATC(1.2) composite polymer membrane.

According to literature, the glass transition temperature T_g of PSU is 185–190 °C [28]. After the pore channels in the PSU membrane are plugged by the PATC phase, another T_g at about 64 °C is observed (Fig. 3). This glass transition temperature reflects the strength of the associative intermolecular interactions between the pendant cation groups, i.e., the strength of ionic complexation, which retards segmental mobility of PTAC chains [29]. On the other hand, two factors are deemed to affect the degree of ionic complexation, namely, the loading extent of the ionic phase and the formation of a branched chain structure [30]. As the polymerization takes place in the confined environment of pore channels, increasing the concentration of the monomer formula results in an even more compact polymerization environment that favours the generation of a branched chain structure. In turn, the branched chains reduce the complexation degree of the ionic groups due to steric blockage. In addition, the complexation degree is related to the specific heat of the ion-conducting phase. The specific heat of a membrane is obtained from the ratio of the area of the endothermic bowl to the mass of the ion-conducting phase contained. As reported in Table 2, they follow the order of PSU-PATC(1.2) ≈ PSU-PATC(1.0) > PSU-PATC(1.5) > PSU-PATC(0.75). This order represents the magnitude of the complexation degree and validates the existence of an optimum loading as a result of the balance between the two factors.

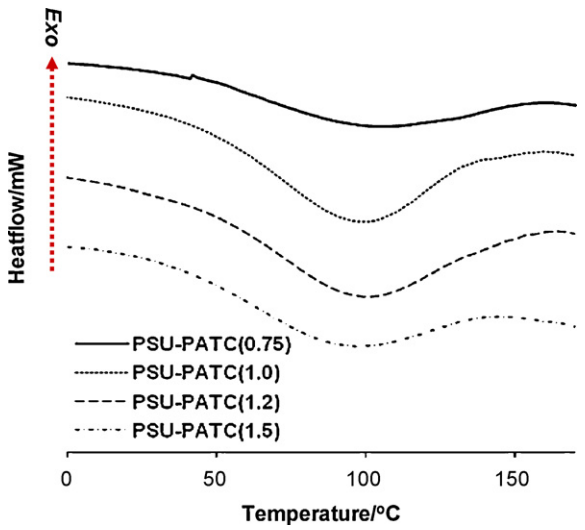

Fig. 3. DSC profiles of PATC-filled PSU membranes.

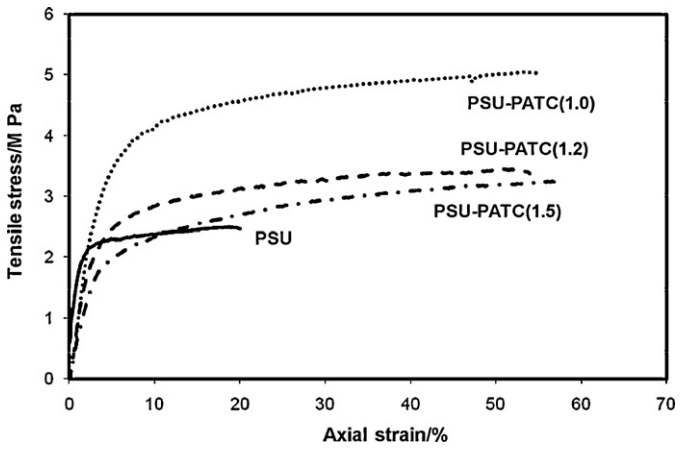

Fig. 5. Mechanical strength of pure porous PSU and pore-filling composite membranes.

The thickness of the fabricated PSU-PATC composite membranes varies from 40 to 60 μm and the cross-sections were examined by FESEM (see Fig. 1s in the Supporting Information). Fig. 4 shows the grid–plug morphology of the membrane matrix that comprises two separate phases: the PSU phase and the PATC phase. Both phases can be discerned at the sub-micrometer level. This is in accordance with the previous thermal analysis results. The ion-conducting phase exhibits an interpenetrating network that is embedded in the prior-formed PSU matrix. Such an interlocking matrix structure can also affect the mechanical properties of the membrane. The tensile stress vs. strain plots of the PSU-PATC membranes (Fig. 5) show that the composite membranes are mechanically stronger than the standalone PSU counterpart. The ion-conducting phase improves the toughness of the membranes, in which the PSU-PATC(1.0) exhibits maximum reinforcement.

3.3. Ion-conducting behaviour of PATC phase

The temperature-dependent ion transport behaviour of the four composite membranes is given in Fig. 6. The magnitude of the conductivity–temperature plots demonstrates the promoting role of ionic complexation. This relation explains the structural requirement for achieving facile ion transport. The ionic complexation provides a series of continuous spatial contacts of the quaternary ammonium cations which serve as sites for the fast hopping of OH^- ions. Finally, evaluation of the membrane in a single H_2/O_2 fuel cell at 60 °C (Fig. 7) allows examination of the response capability of cell voltage to an increase in OH^- flux. It is shown that the maximum power densities of PSU-PATC(1.2) and PSU-PATC(1.5) are approximately 55 and 19 mW cm^{-2}, respectively. Although this order can be predicted from conductivity measurements, the discrepancy in power density describes very different abilities to sustain a high hydroxide ion flux. The effect of ionic complexa-

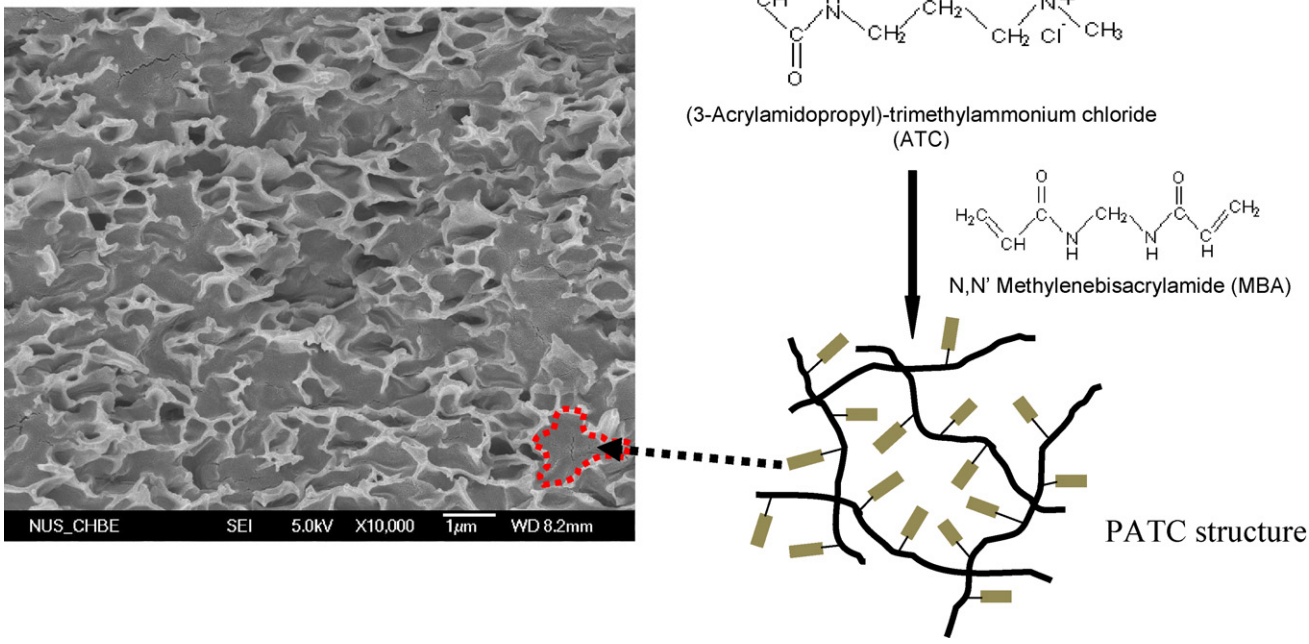

Fig. 4. Cryofractured cross-section of PATC-filled PSU membrane, PSU-PATC(1.2), and schematic illustration of PATC ion-conducting phase.

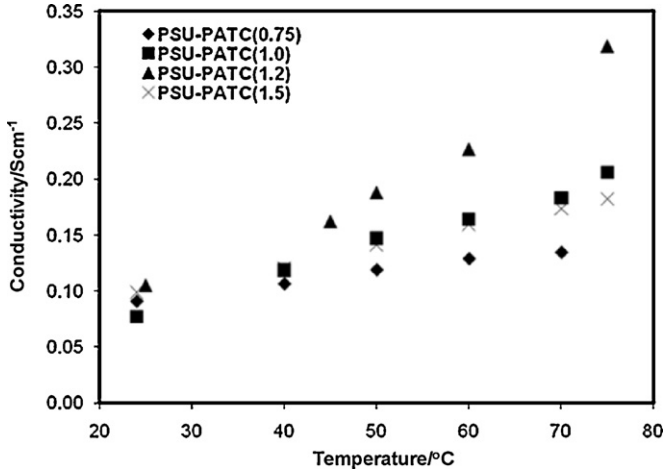

Fig. 6. Influence of temperature on conductivities of composite membranes with filling by different ATC concentration solutions under four-electrode method.

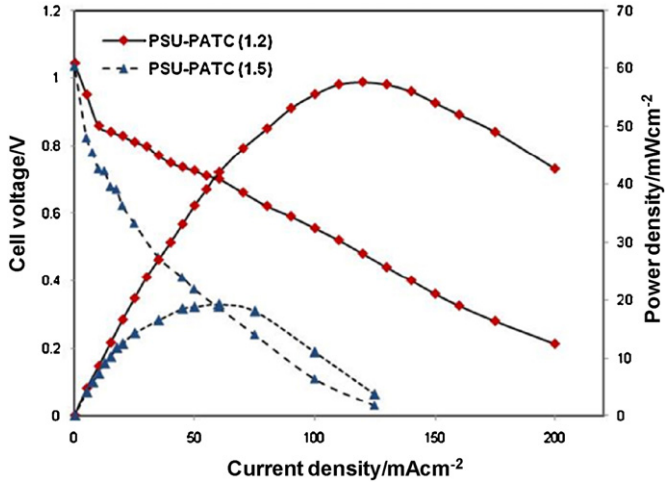

Fig. 7. Electrochemical performances of filled membranes in hydrogen-driven single fuel cell at 60 °C.

tion on cell performance is expected to become more significant at higher temperatures.

4. Conclusions

A novel anion-exchange membrane is fabricated by the pore-filling approach, which is comprised of three consecutive steps: phase-inversion treatment of an as-cast polysulfone membrane to generate interconnected pore channels, filling the pore channels with the monomers, (3-acrylamidopropyl)-trimethylammonium chloride and N,N′-methylenebisacrylamide (1 wt.%), via liquid phase diffusion, and in-situ polymerization of the entrapped monomers. The solvent of the monomer feed plays a crucial role in the pore-filling process. A very mild extent of polymerization in the monomer feed is necessary to facilitate the filling effect. The in-situ polymerization gives rise to a grid–plug microstructure, in which both phases can be discerned at the submicron scale and constitute an interpenetrating network. PSU-PATC(1.2) contains the optimum content of PATC in terms of attaining the maximum degree of ionic complexation. Different preparation conditions result in different degrees of ionic complexation. The PSU-PATC(1.2) membrane, owing to its maximum ionic complexation degree, displays superior capability to uphold a high ion flux compared with the other membranes.

Appendix A. Supplementary data

Supplementary data associated with this article can be found, in the online version, at doi:10.1016/j.jpowsour.2010.12.110.

References

[1] B. Cook, Eng. Sci. Educ. J. 11 (2002) 205–216.
[2] J.R. Varcoe, R.C.T. Slade, Fuel Cells 5 (2005) 187–200.
[3] L.J.M.J. Blomen, M.N. Mugerwa, Fuel Cell Systems, Plenum Press, New York, 1993.
[4] R.C.T. Slade, J.R. Varcoes, Solid State Ionics 176 (2005) 585–597.
[5] M.M. Mench, Fuel Cell Engines, John Wiley and Sons, Hoboken, New Jersey, 2008.
[6] L. Demarconnay, C. Countanceau, J.M. Leger, Electrochim. Acta 49 (2004) 4513–4521.
[7] E. Gulzow, M. Schulze, J. Power Sources 127 (2004) 243–251.
[8] R. Parson, T. VaderNoot, J. Electroanal. Chem. 257 (1988) 9–45.
[9] J. Prabhuram, R. Manoharan, J. Power Sources 74 (1998) 54–61.
[10] A.A. Zagorodni, D.L. Kotova, V.F. Selemenev, React. Funct. Polym. 53 (2002) 157–171.
[11] V. Neagu, I. Bunia, I. Pleasca, Polym. Degrad. Stab. 70 (2000) 463–468.
[12] M.R. Hibbs, M.A. Hickner, T.M. Alam, S.K. McIntyre, C.H. Fujimoto, C.J. Cornelius, Chem. Mater. 20 (2008) 2566–2573.
[13] S. Lu, J. Pan, A. Huang, L. Zhuang, J. Lu, PNAS 105 (2008) 20611–20614.
[14] J.S. Park, S.H. Park, S.D. Yim, Y.G. Yoon, W.Y. Lee, C.S. Kim, J. Power Sources 178 (2008) 620–626.
[15] J. Pan, S. Lu, Y. Li, A. Huang, L. Zhuang, J. Lu, Adv. Funct. Mater. 20 (2010) 312–319.
[16] J. Zhou, M. Unlu, J.A. Vega, P.A. Kohl, J. Power Sources 190 (2009) 285–292.
[17] T.N. Danks, R.C.T. Slade, J.R. Varcoe, J. Mater. Chem. 13 (2003) 712–721.
[18] T.N. Danks, R.C.T. Slade, J.R. Varcoe, J. Mater. Chem. 12 (2002) 3371–3373.
[19] J. Fang, P.K. Shen, J. Membr. Sci. 285 (2006) 317–322.
[20] G. Wang, Y. Weng, D. Chu, D. Xie, R. Chen, J. Membr. Sci. 326 (2009) 4–8.
[21] Y. Xiong, J. Fang, Q.H. Zeng, Q.L. Liu, J. Membr. Sci. 311 (2008) 319–325.
[22] C.C. Yang, J. Membr. Sci. 288 (2007) 51–60.
[23] L. Wu, T. Xu, J. Membr. Sci. 322 (2008) 286–292.
[24] D. Stocia, L. Ogier, L. Akrour, F. Alloin, J.F. Fauvarque, Electrochim. Acta 53 (2007) 1596–1603.
[25] H. Hatori, Y. Yamada, M. Shiraishi, Carbon 30 (1992) 303–304.
[26] M.L. Yeow, Y. Liu, K. Li, J. Membr. Sci. 258 (2005) 16–22.
[27] N. Ma, Y. Yu, Z. Sun, S. Huang, J. Lumin. 126 (2007) 827–832.
[28] S.M. Hong, B.C. Kim, K.U. Kim, I.J. Chung, Polym. J. 23 (1991) 1347–1357.
[29] R.J. Seyler, Assignment of the Glass Transition (STP; 1249), American Society for Testing and Materials, Philadelphia, PA, 1994.
[30] J. Brandrup, E.H. Immergut, E.A. Grulke, A. Abe, R.D. Bloch, Polymer Handbook, 4 ed., John Wiley and Sons, New Jersey, 2005.